UCRL-92793 Revision 1
PREPRINT

Numerical Calculation of Equilibria for the Field-Reversed-Configuration

D. E. Shumaker

This paper was prepared for submittal to
Journal of Fusion Technology

July 1985

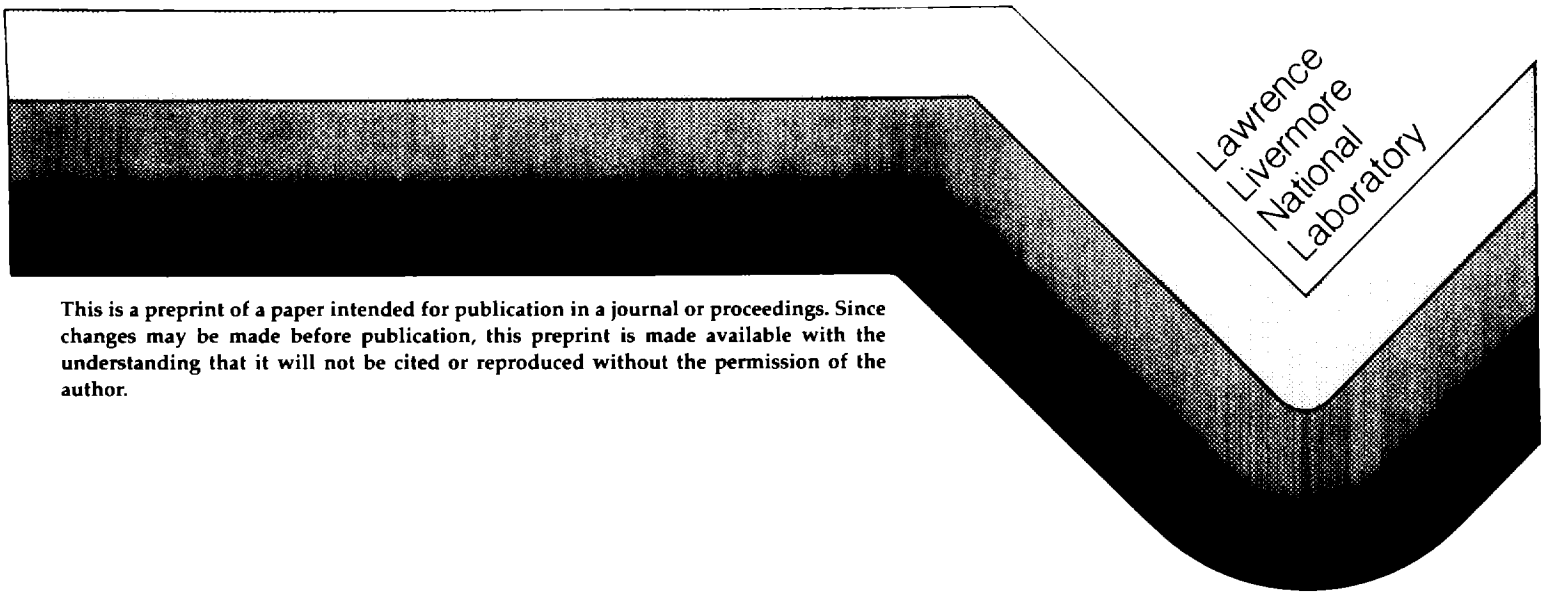

Abstract

A 2-D MHD equilibria code is used to demonstrate how the properties of the equilibria depend on the input quantities. This code uses adiabatic quantities as inputs, which are, entropy and magnetic flux. With the magnetic flux held constant, it is shown that the length of the separatrix is a smooth function of the total entropy. It is shown that the shape of the separatrix can be changed from elliptical to racetrack by changing the profile of the entropy function. This code can also be used for flux and wall compression since the equilibria are determined by adiabatic quantities. Examples of flux and wall compression are presented. An equilibrium is compared with data from the FRX-C experiment.

*Work performed under the auspices of the U.S. Department of Energy by the Lawrence Livermore National Laboratory under contract number W-7405-ENG-48.

I. Introduction

This paper presents a study of field-reversed configuration, FRC, equilibria. A 2-D axisymmetric code is used to compute MHD equilibria. FRCs are elongated compact toroidal plasmas which are formed in theta pinches with a static filling on neutral gas[1]. The FRC contains open and closed field line regions, see Fig. 1. There is no toroidal magnetic field in this calculation. The magnetic field can be written as,

$$\underline{B} = \underline{\nabla}\psi \times \underline{\nabla}\theta \ . \tag{1}$$

The poloidal flux function ψ is the solution of the Grad-Shafranov equation,

$$\underline{\nabla} \cdot \left(\frac{\nabla\psi}{r^2}\right) = - 4\pi \frac{dP}{d\psi} \ . \tag{2}$$

The usual method of computing an equilibrium is to assume that $P(\psi)$ is given and then to solve equation (2) for ψ on a r,z grid. However for the FRC equilibria this approach can become numerically difficult. One of the problems encountered in this direct solution of equation (2) is that the o-point flux, ψ_o is not an input. Also the separatrix length can become a sensitive function of the input parameters[2]. The usual FRC equilibrium is characterized by large pressure gradient near the separatrix. This large pressure gradient can become troublesome when the gradient scale length become comparable to the grid spacing.

An alternate method which will be used in the equilibrium calculations presented here avoids some of these problems. In this method, the equilibrium is specified by adiabatic quantities, instead of assuming that $P(\psi)$ is given. The adiabatic quantity which is used in this code is an entropy function, $\mu(\rho)$,

$$\mu(\rho) = P\left(\frac{dV}{d\rho}\right)^{5/3} , \tag{3}$$

where P is the pressure and V is the volume enclosed by the flux surface labeled by ρ. Also the poloidal magnetic flux function $\psi(\rho)$ is an adiabatic quantity used as an input. The normalized flux coordinate ρ is given by,

$$\rho = \frac{\psi_o - \psi}{\psi_o} , \tag{4}$$

where ψ_o is the value of ψ at the o-point, or $\psi_o = \psi(0)$. ρ has a value of 0 at the o-point, 1 at the separatrix, and is equal to ψ_w/ψ_o at the outer boundary. ψ_w is the value of the flux on the outer boundary. The outer boundary is assumed to be a flux surface. The function $\psi(\rho)$ assigns a flux value to each ρ surface. The $\mu(\rho)$ function is not exactly the entropy, but is conserved in the same way. If $\mu(\rho)$ is multiplied by $\Delta\rho$ it will be proportional to the entropy enclosed by the two surfaces ρ and $\rho+\Delta\rho$.

One of the advantages of using adiabatic quantities is that the o-point flux, ψ_o, is an input quantity. Whereas if $P(\psi)$ is given the ψ_o is a computed quantity. This feature of the adiabatic method allows one to use the experimentally determined ψ_o as an input. Another advantage of using adiabatic quantities is that the separatrix length is not a sensitive function of the

input quantities. This is not the case with other methods which are highly sensitive to inputs[2]. The adiabatic method also eliminates the possibility of bifurcation of the type which have solution with two values of ψ_0 for one input $P(\psi)$[3].

Studies of wall and flux compression are easy when adiabatic quantities are used to determine the equilibrium. An adiabatic flux compression can be simulated by computing a sequence equilibria with the same $\mu(\rho)$ function but different values of ψ on the boundary, ψ_w. A wall compression simulation can be done by again holding $\mu(\rho)$ fixed and computing a sequence of equilibria with different wall radii.

The computer code used in these calculations uses flux surface coordinates. The details of this method is given in Reference (4). The equilibrium calculation is done by solving the Grad-Shafranov equation for ψ on an approximate flux surface grid, using a Galerkin method with triangular finite elements. The boundary value which is used here is that ψ is a constant on the outer wall, ψ_w. At the top of the 2-D region the magnetic field lines are assumed to be parallel to the z axis. This is done by using the boundary condition that $\partial\psi/\partial z = 0$ at the top. With a new value of ψ given on the approximate ψ grid the points are then moved to give a better approximate flux surfaces. This determines a new shape for all internal flux surfaces including the separatrix.

Also since adiabatic quantities are used to determine the equilibrium another step must be added to the iteration procedure. This is the solution of the flux surface average of the Grad-Shafranov equation. This gives a 1-D ODE

which is solved for $V(\rho)$. ψ_0 is used in the solution of this ODE. The boundary conditions used here is that $V(0) = 0$ and $V(1)$ = separatrix volume, which is determined by the 2-D solution. With $V(\rho)$ given, P, which is needed to solve Equation (2), can be obtained from $\mu(\rho)$ using Equation (3).

The equilibrium calculation is an iterative procedure which alternates between the solution of the 2-D Grad-Shafranov equation and the flux surface average of this equation. Convergence is measured by how close the ψ values computed on the finite element grid are to the flux surface label.

One of the advantages of using flux surface coordinates is that the grid spacing can be made small in the regions where the gradients are large. In the FRC these large gradients are localized near the separatrix where the current density is high. With flux surface coordinates the surface spacing can be reduced near the separatrix to obtain better resolution. This is done by having small $\Delta\psi$ for the surfaces near the separatrix.

Also with flux surface cordinates the evaluation of the flux surface averages are easy. No interpolation is necessary to find the location of the flux surfaces. Other method which give ψ on an r,z grid require interpolation to obtain flux surface averages. Flux surface averages are used in the 1-D flux surface averaged Grad-Shafranov equation.

II. Results

In this section results of the FRC equilibrium code are presented. First results are presented which show the dependence of the length of the separatrix on the total entropy. Next a study is presented of the effect of the entropy profile on the shape of the separatrix. Two compression studies are then presented. Finally a comparison is given of experimental interferometry data with an equilibrium calculation for the FRX-C experiment.

Figure 2 illustrates the dependence of the separatrix length, ℓ_s, and the separatrix radius, r_s, on the total entropy enclosed by the separatrix, M_{Int}, defined by,

$$M_{Int} = \int_0^1 \mu(p)\, d\rho \qquad (5)$$

All other input quantities are held constant. There are two sets of data presented in this figure. One is for a straight cylinder flux conserver, solid points, and one set for a flux conserver with a passive mirror coil. In this case the outer coil has a smaller diameter on the ends. The coil dimensions in this set of calculation are similar to the FRX-C experiment at LANL.

As can be seen in Fig. (2) the separatrix radius is approximately independent of the total entropy. This statement is only true as long as the FRC is elongated. For the case without the passive mirror the separatrix lenght, ℓ_s, is approximately a straight line on the log-log plot. For the case with the mirror coil the ℓ_s is reduced when the plasma begins to lean against the mirror field. Also the separatrix radius is increased slightly.

Figure 3 illustrates the dependence of the shape of the separatrix on the $\mu(\rho)$ function. These examples have the same total entropy. The form of the input function for these four cases are, from left to right, $\sqrt{1-\rho}$, $(1-\rho)$, $(1-\rho)^2$ and $(1-\rho)^4$. The equilibria with the large gradient of $\mu(\rho)$ near the separatrix tend to have separatrix with an elliptical shape. The $\mu(\rho)$ profiles which are more peaked near the o-point tend to produce the more racetrack shaped separatrix. Also note that the volume of the inner most flux surface tends to be larger for the peaked $\mu(\rho)$. This is expected since the larger entropy enclosed by the inner flux surfaces will expand these flux surfaces. Also note that the current density near the separatrix is more peaked for the elliptical shaped flux surfaces.

Figure 4 illustrates an adiabatic wall compression sequence in which all input are held constant except for the radius of the wall r_w. In this figure three equilibria are presented with wall radii of 15, 20, and 30 cm. Reference (5) gives the dependence of separatrix length, ℓ_s, and the magnetic field at the wall, B_w, on the wall radius, r_w,

$$\ell_s \, r_w^{-0.4} \approx \text{constant} \tag{6}$$

$$B_w \, r_w^2 \approx \text{constant} \tag{7}$$

$$\chi_s \approx \text{constant} \, , \tag{8}$$

where $\chi_s = r_s/r_w$. The results from the computed equilibria agree with these expression within 1%. The $\mu(\rho)$ used in these calculations is proportional to $(1 - \rho)$, which is zero on the separatrix.

Figure 5 illustrate an adiabatic flux compression sequence. In this set of equilibria the only input which is changed is the flux on the outer wall. The sequence would correspond to an experiment where the current in the pinch coil is increased. The calculation would be appropriate for an experiment where the current is increased faster than any transport processes across the field lines but slow enough that temperature equilibration along the field does occur. As can be seen flux compression changes both the separatrix lenght, ℓ_s, and the separatrix radius, r_s. Flux compression produces a flatter pressure profile and a current profile which becomes more peaked near the separatrix. The $\mu(\rho)$ used in these calculations is proportional to $(1 - \rho)$.

Simple expression similar to equations (6), (7) and (8) do not exist for flux compression. The evolution of the compression depends on the details of the initial profiles. Reference (5) gives expression similar to Equations (6), (7) and (8) only for limiting forms of the pressure profile. The ℓ_s and B_w for the flux compression given in Figure 5 are within 7% of the "high flux sharp boundary" model given in Reference 5.

Figure 6 gives an equilbrium which was produced to model the FRX-C experiment at LANL[6]. The dependence illustrated in Figures (2), (3) and (5) are helpful in producing an equilibria with the desired parameters. By changing the external flux, ψ_w, or the internal flux, ψ_o, the separatrix radius, r_s, can be matched to the desired value. Information of this sort is given in Figure 5, (or a similar set for different values of r_w). With r_s set the separatrix length is matched by changing, M_{INT}, Equation (5). Then the separatrix shape can be charged by varying the $\mu(\rho)$ profile. To match the experiment some plasma pressure must be added in the open field line region.

This is done by adding and exponential decreasing $P(\psi)$ in this region, based on the value of $P(\psi)$ just inside of the separatrix. Figure 7 gives a comparison of experimental side-on interferometry data[7] with the same quantity computed from the equilibrim shown in Figure 6. In this calculation the electron and ion temperature are assumed to be constant in space. This assumption is necessary to obtain a density profile from the given pressure profile.

In summary, it has been demonstrated that the FRC equilibrium code can compute equilibrium with a large range of parameters. Also by adjusting the inputs equilibrium similar to experiments can be computed.

References

(1) W.T. Armstrong, R.K. Linford, J. Lipson, D.A. Platts, and E.G. Sherwood, Phys. Fluids 24, p. 2068 (1981).

(2) D.W. Hewett and R.L. Spencer, Phys. Fluids, p. 1299 (1983).

(3) B. Marder and H. Weitzner, Plasma Phys. 12, p. 435 (1970).

(4) D.E. Shumaker, J. Comput. Phys. 53, p. 456 (1984).

(5) R.L. Spencer, M. Tuszweski and R.K. Linford, Phys. Fluids 26, p. 1564 (1983).

(6) R.E. Siemon, W.T. Armstrong, R.R. Bartsch, R.E. Chrien, J.C. Cochrane, R.W. Kewish, P.O. Klingner, R.L. Linford, J. Lipson, K.F. McKenna, D.J. Rei, E.G. Sherwood and M. Tuszewski, Plasma Physics and Controlled Nuclear Fusion Research, Ninth Int. Conf. Baltimore (1982).

(7) R.L. Spencer and M. Tuszewski, Phys. Fluids 28, p. 1810 (1985).

Figures

(1) FRC Equilibrium

(2) Dependence of separatrix lenght, ℓ_s, and separatrix radius, r_s, on the total entropy enclosed by the separatrix, M_{INT}. Solid points are for equilibria without passive mirror. Open points are for equilibrium with passive mirror.

(3) Dependence of separatrix shape on the entropy function profile $\mu(\rho)$. Each column corresponds to a different equilibria. The input function $\mu(\rho)$ is given in the second row.

(4) Wall compression simulation. Each column corresponds to a equilibrium with a different wall radius, r_w.

(5) Flux compression simulation. Each column corresponds to a different flux enclosed by the outer boundary, ψ_w.

(6) FRX-C equilibrium. (a) Flux surfaces, (b) Poloidal flux vs r at z = 0, (c) Pressure vs r at z = 0, (d) Magnetic field vs r at z = 0, and (e) Current density vs r at z = 0.

(7) Comparison with side-on interferometry data. Line is from simulation, points are experimental data[7]. (a) Line integral of density, normalized, vs, chord, d, at midplane, z = 0, and end z = 90 cm. (b) Line integral of density, normalized, vs, z aat d = 0.

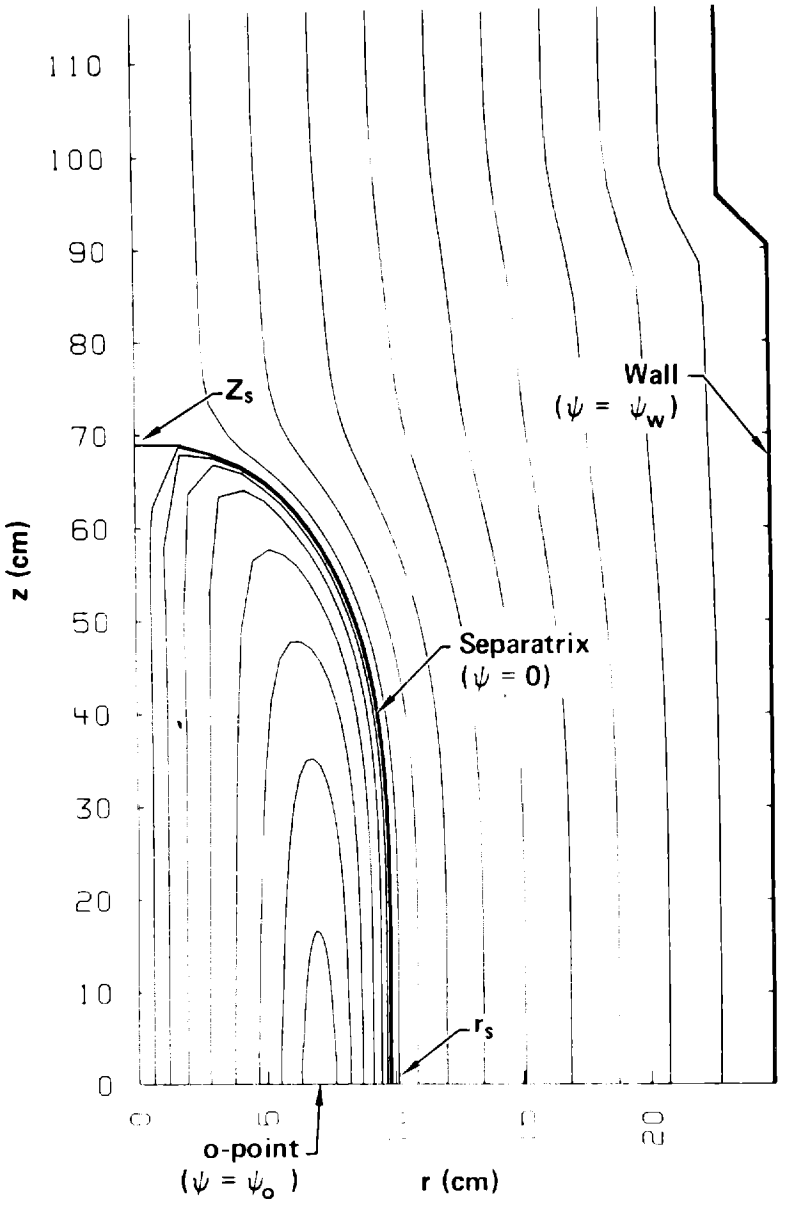
110
100
90
80
70
60
50
40
30
20
10
0
z (cm)
Z_s
Wall
($\psi = \psi_w$)
Separatrix
($\psi = 0$)
r_s
o-point
($\psi = \psi_o$)
r (cm)

Figure 1

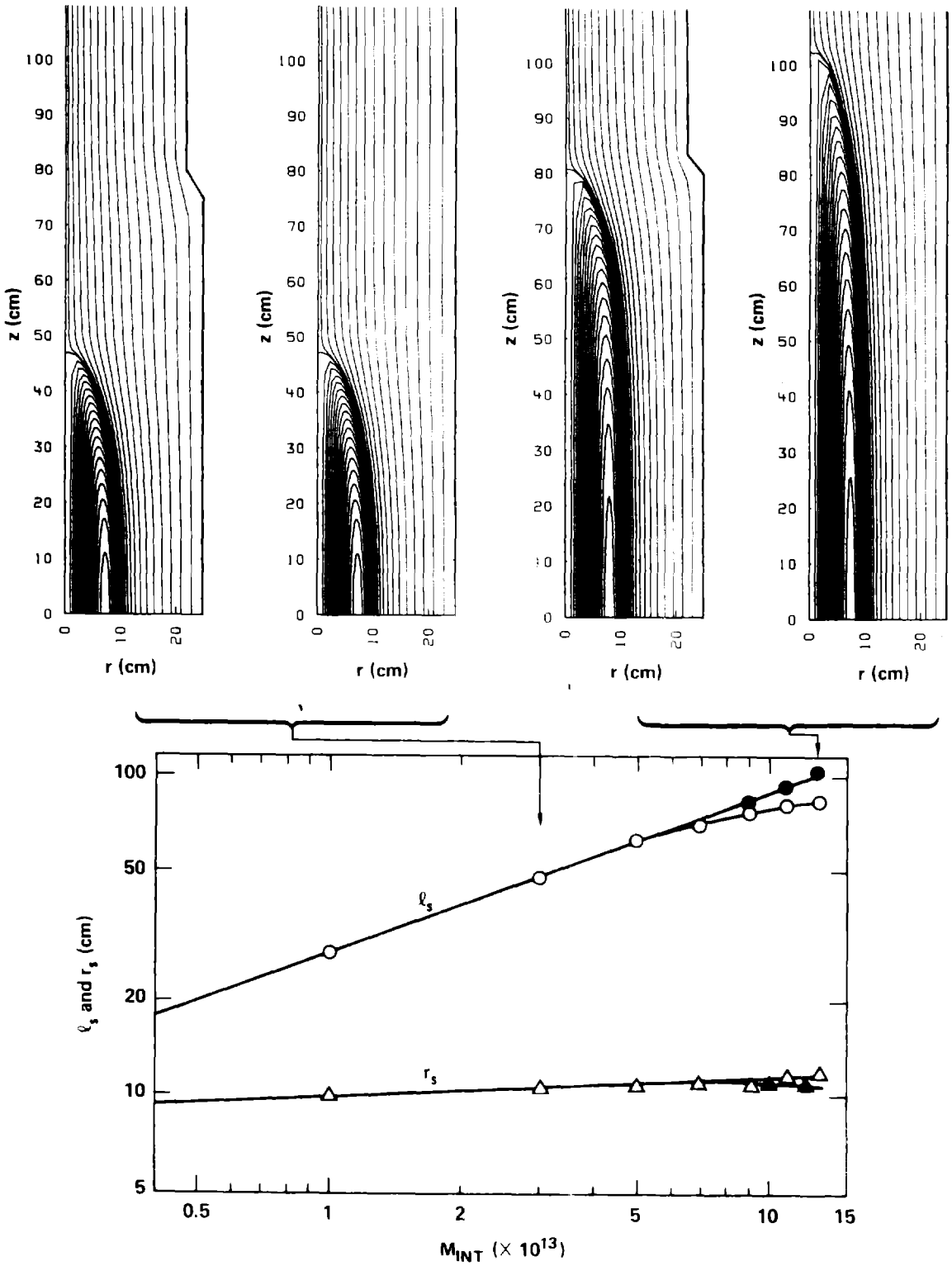

Figure 2

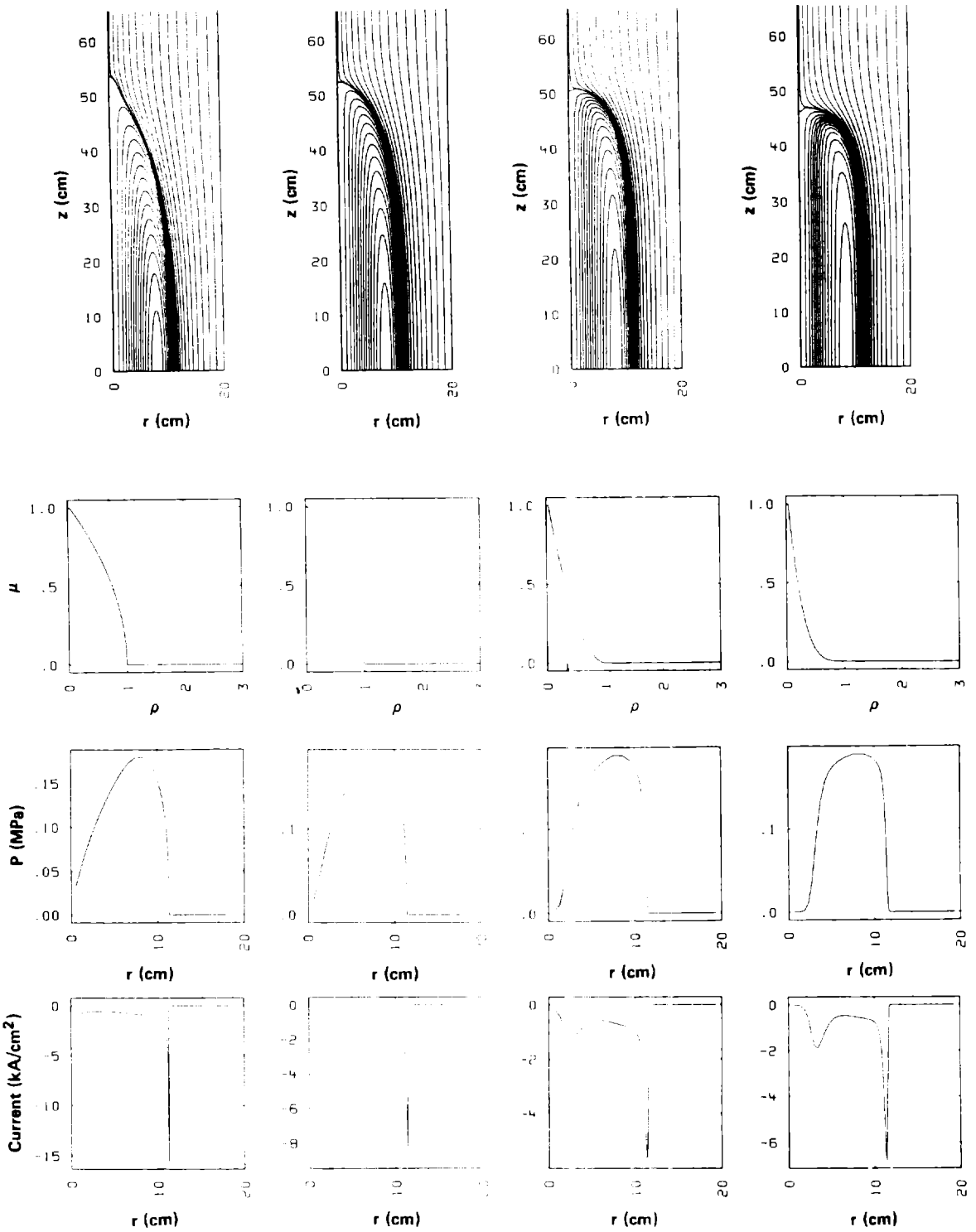

Figure 3

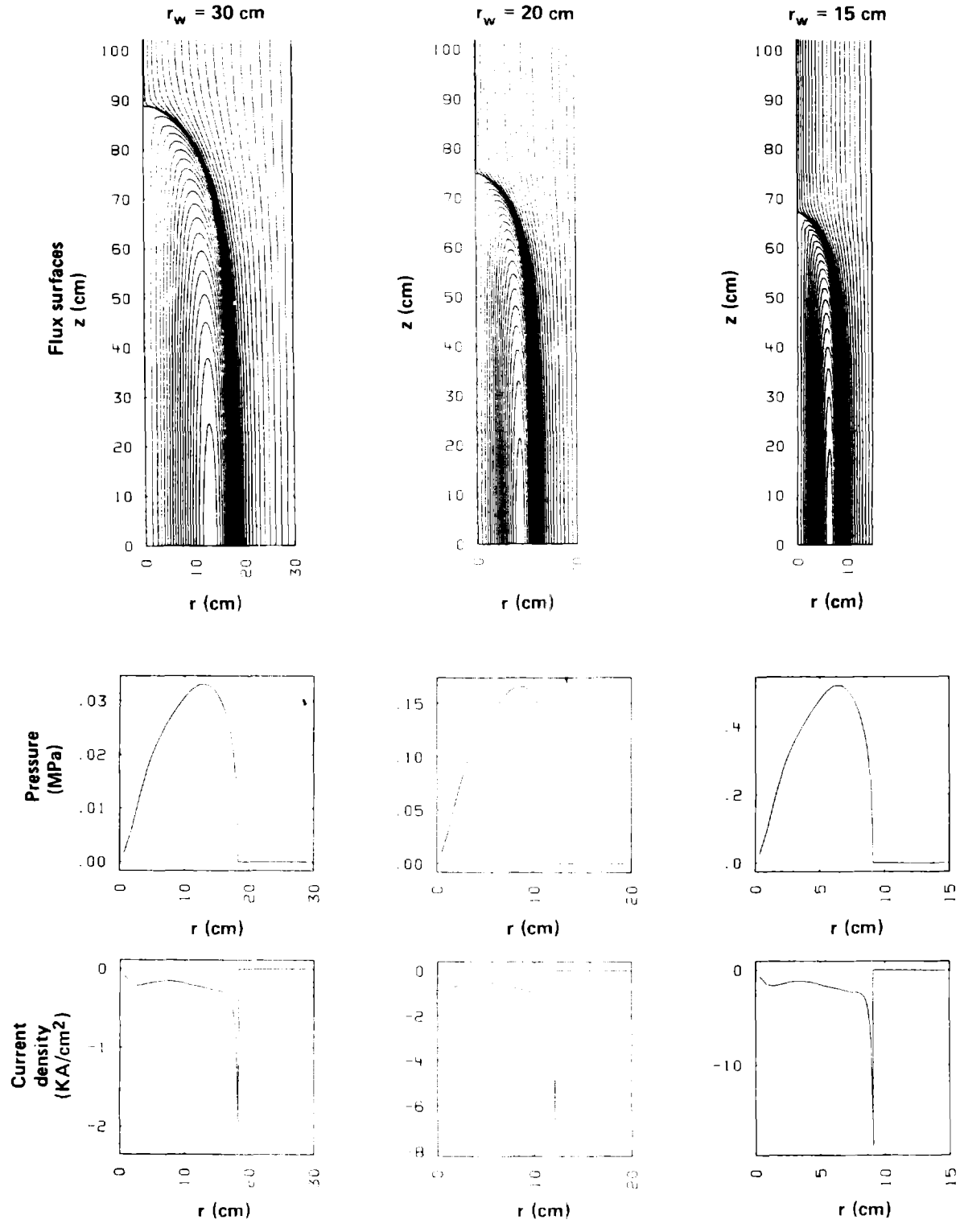
r_w = 30 cm
r_w = 20 cm
r_w = 15 cm
Flux surfaces
z (cm)
z (cm)
z (cm)
r (cm)
r (cm)
r (cm)
Pressure
(MPa)
r (cm)
r (cm)
r (cm)
Current
density
(KA/cm^2)
r (cm)
r (cm)
r (cm)

Figure 4

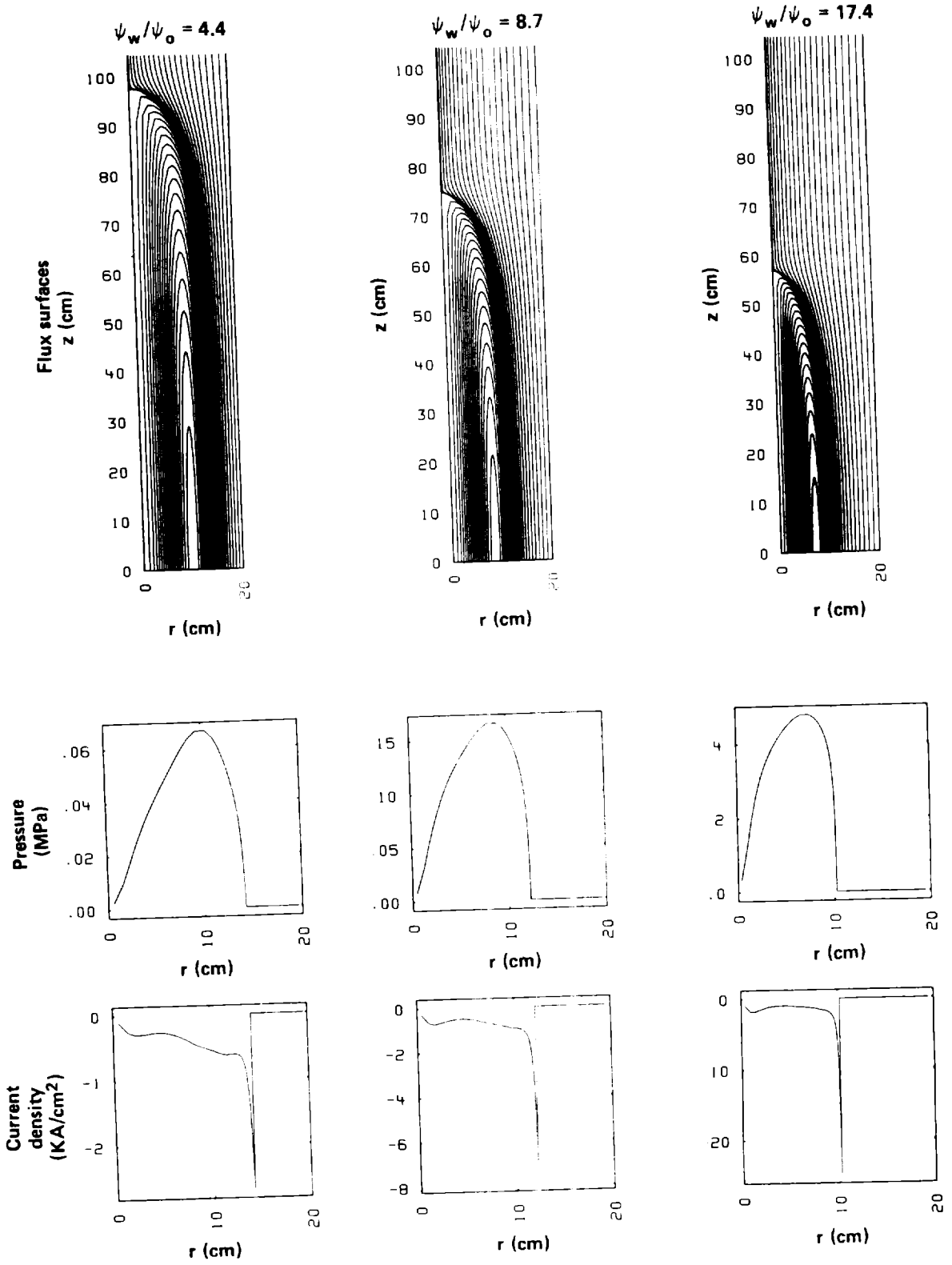
ψ_w/ψ_o = 4.4
ψ_w/ψ_o = 8.7
ψ_w/ψ_o = 17.4
Flux surfaces
z (cm)
r (cm)
Pressure
(MPa)
Current
density
(KA/cm^2)

Figure 5

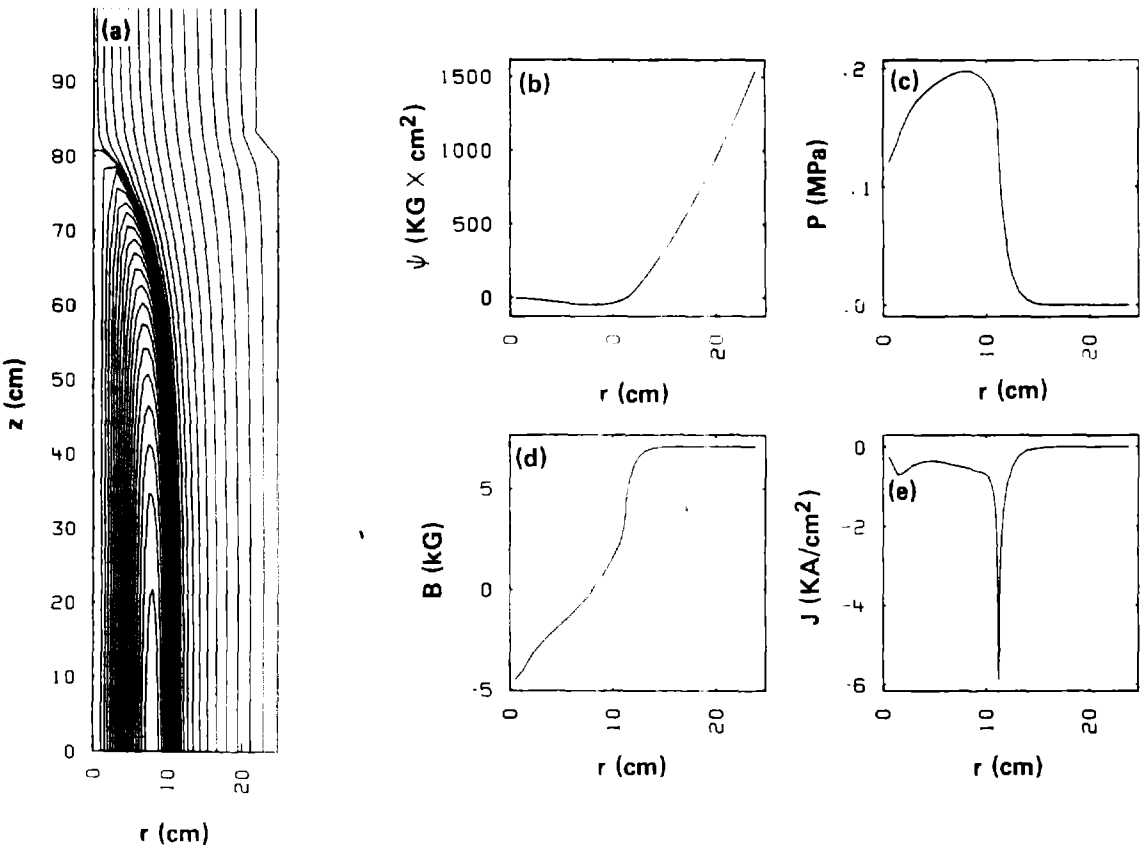

Figure 6

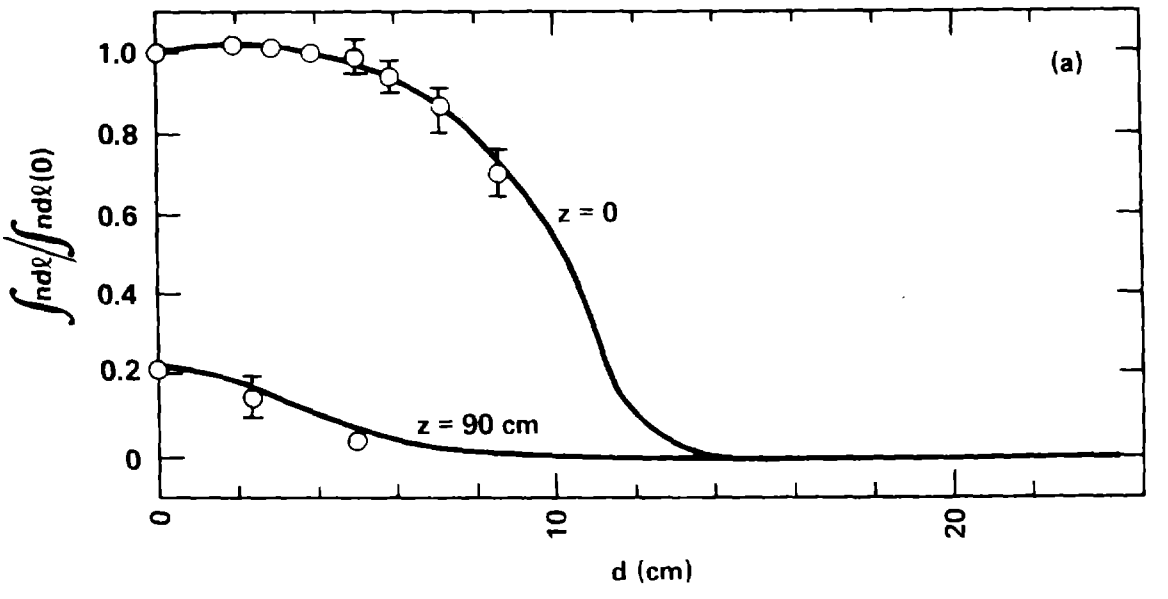
(a)
1.0
0.8
0.6
0.4
0.2
0
z = 0
z = 90 cm
0
10
20
d (cm)
$\int ndl / \int ndl(0)$

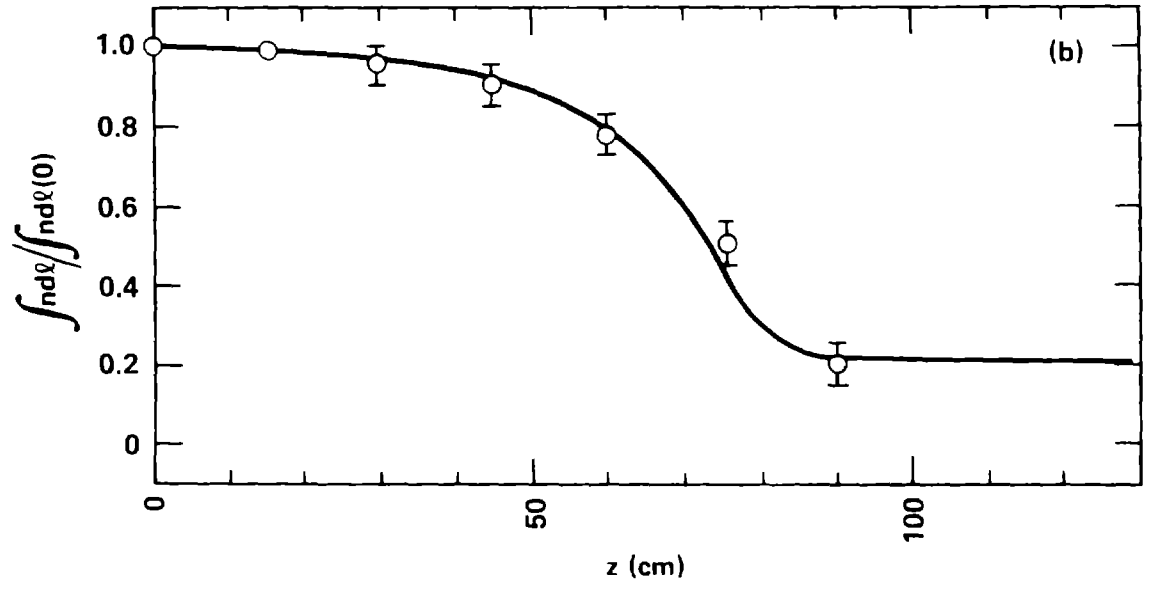
(b)
1.0
0.8
0.6
0.4
0.2
0
0
50
100
z (cm)
$\int ndl / \int ndl(0)$

Figure 7